8—9

Peg-Free Hand Geometry Recognition Using Hierarchical Geometry and Shape Matching

Alexandra L.N. Wong[1] and Pengcheng Shi[2]
Department of Electronic and Electrical Engineering
Hong Kong University of Science and Technology

Abstract

We propose a feature-based hierarchical framework for hand geometry recognition, based upon matching of geometrical and shape features. Rid of the needs for pegs, the acquisition of the hand images is simplified and more user-friendly. Geometrical significant landmarks are extracted from the segmented images, and are used for hand alignment and the construction of recognition features. The recognition process is hierarchical in nature, and it employs a Gaussian Mixture Model for the first group of features, followed by a distance metric classification of the second group of features if necessary. The method has been tested on a medium size dataset of 323 images with promising results of 89% hit (true acceptance) rate and 2.2% false acceptance rate.

1 Motivation

Biometrics is getting more and more attention in recent years for security and other purposes. So far, only fingerprint has seen limited success for on-line security check, since other biometrics verification and identification systems require more complicated and expensive acquisition interfaces and recognition processes.

Hand geometry has long been used for biometric verification and identification because of its acquisition convenience and good verification and identification performance [1, 2, 3, 4, 5]. From anatomical point of view, human hand can be characterized by its length, width, thickness, geometrical composition, shapes of the palm, and shape and geometry of the fingers. Earlier efforts have used combinations of these features for recognition with varying degrees of success. Traditionally, pegs are almost always used to fix the placement of the hand, and the length, width and thickness of the hand are then taken as features [2, 3, 4]. In [5], the outline of the hand is extracted and is represented by a group of salient points, which serve as features in the verification process.

Even though the pegs often cause deformation on hand geometry, which in turn reduces the accuracy in feature extraction and further analysis, they are used extensively to fix the hand placement during image acquisition. In general, the use of pegs introduces two problems. First, as shown in Figure 1, pegs will almost definitely deform the shape of the hand. Second, even though the pegs are fixed, the fingers may be placed differently at different instants, and this causes variability in the hand placement as illustrated in Figure 1. These problems will degrade the performance of hand geometry verification because they adversely affect the features.

Figure 1. Three peg-fixed hand photos: deformed hand shape (left), different placements of the same hand (middle and right).

In this paper, we present a novel recognition system that uses a peg-free hand image acquisition and a hierarchical geometry (length and width of the fingers) and shape (length and location of the fingertip regions) matching for user identification. Without the needs for pegs, the system has simple acquisition interface. Users can place their hands in arbitrary fashion and can have various extending angles between the five fingers. Geometric significant shape landmarks are extracted from the segmented images, which are further used for hand alignment and hand geometry recognition. Our system offers a simple and friendly acquisition interface and a good recognition rate with low false acceptance rate.

2 Methodology

2.1 Hand Image Acquisition

A commercial flatbed scanner was used to acquire the hand images. Randomly placed hands of the participants were scanned with dark background using 150dpi scanning quality. The fingers must be clearly separated from each other in the image in order to obtain a complete hand shape. Examples of acquired hand images are shown in the top row of Figure 2.

Address: Department of Electronic and Electrical Engineering, Hong Kong University of Science and Technology
Clear Water Bay, Kowloon, Hong Kong. Tel: +852 2358 8529 Fax: +852 2335 0194 E-mail: [1]**alex@ust.hk**; [2]**eeship@ust.hk**

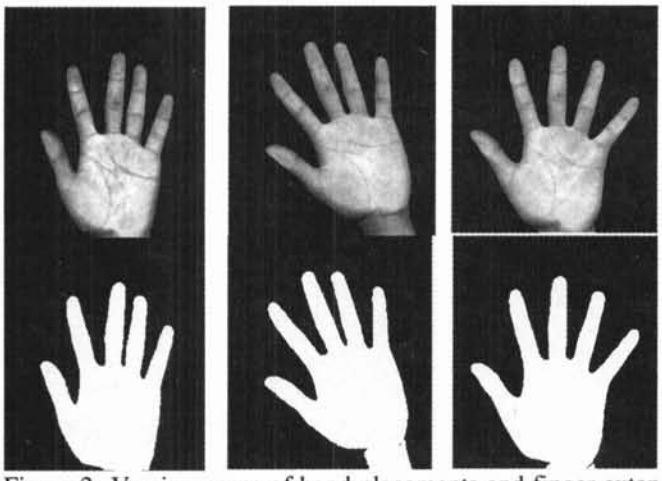

Figure 2. Varying poses of hand placements and finger extension angles from peg-free acquisition. Top: typical (left), palm rotation (middle), and widely extended fingers (right). Bottom: corresponding binary images.

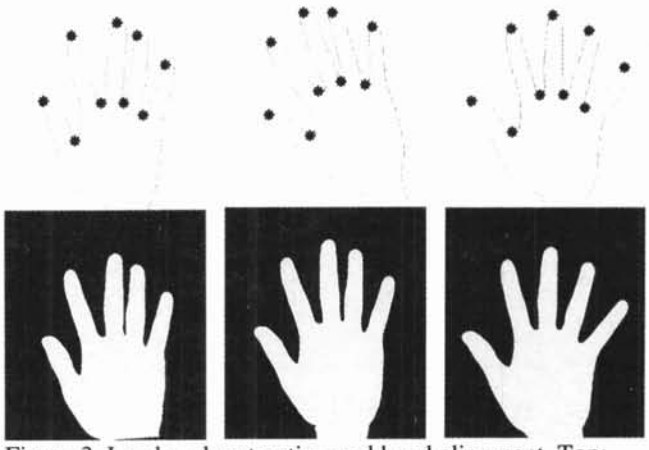

Figure 3. Landmark extraction and hand alignment. Top: extracted hand boundary and landmarks. Bottom: aligned images such that all the middle fingers are vertically upward.

2.2 Landmark Extraction and Hand Alignment

Since there is clear distinction in intensity between the hand and the background by design, a binary image is obtained through thresholding (Figure 2) and hand boundary is easily located afterwards (Figure 3). Geometrical landmarks, i.e. the fingertip points and the valley points between adjacent fingers, are extracted by traveling along the hand boundary and searching for curvature extremities.

A border following algorithm is applied to locate the boundary of the binary image [6]. For each boundary point (x, y), its curvature K is estimated from:

$$K = \frac{\left(x'y'' - y'x''\right)^2}{\left(x'^2 + y'^2\right)^{3/2}}$$

where y', x', y'', and x'' is the first- and second-order coordinate changes along y and x, calculated from the neighboring points of (x, y). From the calculated curvature information, nine landmarks are located which are curvature extremities, as shown in top row of Figure 3.

These landmarks, instead of the traditional pegs that often cause hand deformation [2, 3, 4, 5], are used to align the palm to vertical displacement. A reference point and a reference axis are found first. The middle finger baseline is created by connecting the second and third valley points. The mid-point of this baseline is used as the reference point of the palm rotation, and the axis from the reference point to the middle fingertip landmark is selected as the reference axis. A rotation angle is thus calculated from the orientation of the reference axis:

$$\theta = \tan^{-1}\left(\frac{\Delta y}{\Delta x}\right)$$

The reference axis is aligned to be upward vertical in order to align the hand image with the database template to the same orientation, and finger-wise correspondence between the input image and the template is established, using the rotation equation:

$$\begin{bmatrix} x_{new} \\ y_{new} \end{bmatrix} = \begin{bmatrix} \cos\theta & \sin\theta \\ -\sin\theta & \cos\theta \end{bmatrix} \begin{bmatrix} x \\ y \end{bmatrix}$$

The aligned images are shown in bottom row of Figure 3.

Compared to the traditional peg-fixed acquisition, our method is less sensitive to the placement of the hand, and is more user-friendly and convenient.

2.3 Feature Selection

Salient features are necessary for the robust recognition of hand geometry. As shown in Figure 4, the lengths of the five fingers (L_1 to L_5), the widths of the four fingers (except the thumb) at two locations (W_1 to W_8), and the shape of the three middle fingertip regions (S_1 to S_3) are selected for our system.

Finger baselines: As illustrated in Figure 4, four between-finger valley points are located on the hand boundary.

- Because the middle-finger is the only finger which does not have large spatial variations of its valley points for different placement of the hands, the middle-finger baseline is formed by connecting the second and third (count from the left) valley points.
- The ring finger has two valley points (third and fourth) as well. However, since the relative heights of these two valley points are more sensitive to hand placement, it is unstable to use these two valley points to form the baseline for the ring finger.
- The baselines for the thumb, the index finger, the ring finger, and the little finger are formed in the same fashion. We assume that the two end points of each baseline have the same distance from the respective fingertip point. Using one of the respective valley points as one of the end points (first valley point for thumb, second for index, third for ring, and fourth for

pinky), we locate the other end point by searching for the point which has the same distance from the fingertip at the another side of the boundary of the finger. The baselines are formed afterwards by connecting pairs of end points.

Finger lengths: For each finger, the fingertip point and the middle point of its baseline determine its finger length L_i, i=1,2,3,4.

Finger widths: For each finger except the thumb, the first finger width W_i, i=1, 3, 5, 7, is the width at the middle point of the finger length, and the second finger width W_j, j=2, 4, 6, 8, is the width at one-eighth way (with respective to the finger length) from the fingertip.

Fingertip regions: For the index, middle, and ring fingers, the top one-eighth portion of the fingers are defined as the fingertip regions. Each fingertip region is represented by a set of ordered boundary points (between 50 to 90). The bottoms of the fingertip regions are coincident with W_2, W_4, and W_6 respectively. Similar to the palm alignment, the fingertip regions are also aligned by the method we mentioned in section 2.2. The middle point of the bottom line is found as the reference point and the axis between middle point and the fingertip top point is the reference axis. As long as the rotation angle is found, the fingertip regions are aligned. The coordinates of the fingertip points are recorded, and re-sampling may be required in order to match the testing image fingertip points and the template fingertip points.

2.4 Hierarchical Recognition

The extracted hand features are put into two groups. Group #1 consists of the 13 finger lengths and widths of all fingers, and group #2 consists of the 3 fingertip regions. A sequential recognition scheme is adopted, using these two groups of features.

Group #1: A Gaussian mixture model (GMM), based upon statistical modeling and neural networks [2, 3], is used to obtain the characteristic parameters for the group #1 features of each person:

$$p\left(\vec{x}/u\right)=$$

$$\sum_{i=1}^{M}\frac{c_i}{(2\pi)^{L/2}\left|\Sigma_i\right|^{1/2}}\exp\left\{-\frac{1}{2}\left(\vec{x}-\vec{\mu_i}\right)^T\Sigma_i^{-1}\left(\vec{x}-\vec{\mu_i}\right)\right\}$$

where c_i is the weighting coefficient of each of the Gaussian model, μ_i is the mean vector of the each model, Σ_i is the covariance matrix of each model, M is the number of the models, and L is the dimension of the feature vectors. The GMM is trained by the training images of each person, and the characteristic parameters are acquired for each user in terms of c_i, μ_i, and Σ_i of size 1x M. The probability $p(\vec{x}/u)$ of an input test image $\vec{x}$ belongs to class u can then be calculated with the above equation.

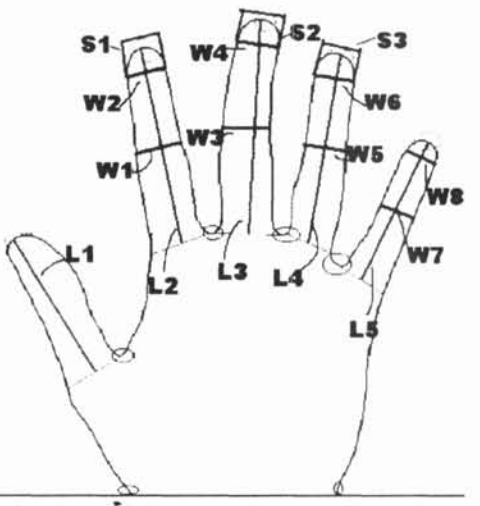

Fig.4. Definitions of the hand features: finger length L_i (i=1,...,5), finger width W_j (j=1,...,8), and fingertip region S_k (k=1,...,3).

If the image is determined to pass a preset threshold of the GMM probability estimation of the template (we set the passing probability threshold to be 0.5 for our experiment), the image is further processed with the group #2 features in the following step.

Group #2: The mean distributions of the group #2 features, the point distributions of the three fingertip regions, are used as the fingertip templates for each user in the database. The number of points on the input fingertip region S_k and on the corresponding template T_{S_k} must be the same, and linear re-sampling of S_k is needed if the two are different but the difference is within an acceptable range (10% in our implementation). If the difference is greater than 10%, it is rejected.

For each fingertip point (x_i, y_i) on S_k, it is classified as either a failure point or a hit point, which is determined by an Euclidean distance measure between (x_i, y_i) and its corresponding template point $(x_{i_{temp}}, y_{i_{temp}})$ on T_{S_k}:

$$D_i=\sqrt{\left(x_i-x_{i_{temp}}\right)^2+\left(y_i-y_{i_{temp}}\right)^2}$$

If the distance is larger than certain threshold (we have set it to 2 pixels), it is a failure point. Otherwise, it is a hit point.

For all the fingertip points of the three fingertips, we calculate the percentage of failure points. If the percentage is higher than another threshold (say, 10%), we declare that the input hand image does not correspond to the template and should be rejected. Otherwise, it is recognized as the valid user represented by the template.

	only using Group #1	*Group #1 + Group #2*
Hit Rate	1	0.8889
FAR	0.1222	0.022

Table 1. The hit rate and FAR for the testing images using group #1 feature and GMM only, and using the hierarchical recognition scheme of group #1 and group #2 features

3 Experiment and Discussion

323 right-hand images, grouped into two datasets, are used in our testing experiment of the system. The first set of data contains totally 288 training and testing images of 22 people, 12 to 15 images each. After the extraction of the landmarks and alignment of the hand orientation, recognition features for each input image are computed and grouped. For each person, 9 images are used for GMM training and template calculation, and the rest are used as test images (90 in total). The second set of the data contains 35 test images from 7 people, each with 5 images. This set of data is used to test the effects of the thresholds on the hit rate and false accept rate (FAR).

For an input testing hand image from the first dataset, its group #1 features are calculated. If this group of features possesses a passing probability on the GMM testing (greater than 0.5) against any template out of the 22 templates in total, its group #2 features are constructed and we move on to the next stage of recognition. We set the threshold on the difference of the number of points heuristically to be 10% as mentioned earlier. If the input image can pass this test, we move to the final step where the distance for hit point is set at 2 pixels, and the failure percentage threshold is set at 10%. If the image can pass this test, it is recognized as the user represented by this template.

Table 1 shows the hit rate for using group #1 features only and for using both group #1 and group#2 with heuristic thresholds. For group #1 only, the hit rate is 1 and the FAR is 0.1222, which is quite high as well. If using both group #1 and #2 features, as in our hierarchical recognition system, the hit rate drops to 0.8889 and the FAR decreases to 0.022. For security system, low FAR is often essential, even at the cost of lower hit rate.

Using the second set of data, which contains 35 hand images of impostors who are not in the training set, we observe the distributions of the GMM probability measure, the input-template point number difference, and the failure percentage. From this particular test, we conclude that the GMM threshold plays an important role in reducing the FAR, and the thresholds for the point number difference and the failure percentage further make sure the false acceptance is minimized. Figure 5 shows a ROC curve which reflects the impact of the GMM threshold.

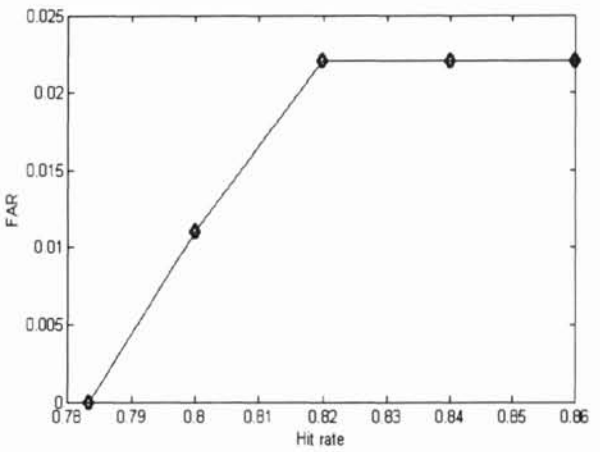

Fig.5. ROC curve by adjusting GMM passing threshold.

Compared to peg-fixed hand geometry recognition systems, our system has an acceptable hit rate (true accept rate) of 88.89% with low FAR at 2.22%. In [2,3], GMM is used as the training model for the length and width of the hand geometry, and has achieved higher hit rate at 96% but with higher 4.9% FAR as well. Further, it has constrained hand placement because of the need for pegs.

The hand geometry recognition system can be further combined with other hand biometrics for better performance. Since the acquisition is done by a commercial flatbed scanner, by adjusting the scanning resolution and brightness, we can acquire the palm print from the hand images as well. A multi-biometrics recognition system is under development.

References

[1] J. Ashbourn, *Biometrics: Advanced Identity Verification*, Springer-Verlag, New York, 2000.

[2] R. Sanchez-Reillo, "Hand geometry pattern recognition through Gaussian mixture modeling", in *15th International Conference on Pattern Recognition,* Vol.2, Sep, 2000. Pp. 937-940.

[3] R. Sanchez-Reillo, C. Sanchez-Avila, and A. Gonzalez-Marcos, "Biometric Identification Through Hand Geometry Measurements", *IEEE Transactions on Pattern Analysis and Machine Intelligence,* **22**(10), 2000. Pp: 1168-1171.

[4] A.K. Jain, A. Ross, and S. Pankanti, "A Prototype Hand Geometry-based Verification System", *2nd International Conference on Audio- and Video-based Biometric Person Authentication*, Mar, 1999. Pp. 166-171.

[5] A.K. Jain and N. Duta, "Deformable matching of hand shapes for verification", in *IEEE International Conference on Image Processing*, Oct, 1999. Pp. 857-861

[6] A. Rosenfeld and A.C. Kak, *Digital Picture Processing*, Academic Press, San Diego, 1982.